Cite this article
Fang K and Fall M (2022)
Shear characteristics of the rock/cemented tailings interface exposed to sulfate attack.
Geotechnical Research **9(4)**: 186–195,
https://doi.org/10.1680/jgere.22.00017

Research Article
Paper 2200017
Received 04/03/2022; Accepted 06/06/2022
Published online 07/09/2022
Published with permission by the ICE under the
CC-BY 4.0 license.
(http://creativecommons.org/licenses/by/4.0/)

Geotechnical Research

ice Publishing

Shear characteristics of the rock/cemented tailings interface exposed to sulfate attack

Kun Fang PhD
Department of Civil Engineering, University of Ottawa, Ottawa, ON, Canada

Mamadou Fall PhD
Department Chair, Department of Civil Engineering, University of Ottawa, Ottawa, ON, Canada (corresponding author: mfall@uottawa.ca)

A clear understanding and accurate assessment of the mechanical properties of the interface between backfill material and the adjacent rock mass is paramount to a safe and economical design of cemented paste backfill (CPB) structures. With the CPB being a cementitious material, sulfate compounds prevalent in the mining environment may affect the shear characteristics of the CPB–rock interface. However, there are currently no research studies on the long-term shear behaviour of the CPB–rock interface exposed to sulfate attack, although CPB often contains a relatively large amount of sulfate ions. This paper presents and discusses the findings obtained through experimental investigation of the impact of the initial sulfate concentration in CPB on the shear characteristics of the interface between rock and CPB cured for long durations. The obtained results show that sulfate considerably influences the long-term shear strength and behaviour of the interface. Sulfate can either negatively or positively alter the shear properties of the mature CPB–rock interface due to the competition between the processes that reduce or increase the strength at the interface. The dominant process is a function of the initial sulfate content and the curing time.

Keywords: interfaces/Portland cement/shear strength/sustainability/tailings

Introduction

Cemented hydraulic backfill (CHB), cemented rock backfill (CRB) and cemented paste backfill (CPB) are the three main types of cemented backfills that are used in underground mining operations. CHB is produced by mixing mill tailings (with 60–75% solid content) and cement, while CRB contains waste rock, tailings and a small fraction of cement (Amaratunga and Yaschyshyn, 1997). However, due to the potential geotechnical hazards associated with CHB (e.g. failure of backfill barricades) and its higher cost, the use of CHB has been increasingly restricted. In contrast, CPB is becoming more popular as a preferred backfill material or technology in recent years (Brackebusch, 1995; Hassani and Archibald, 1998). CPB, a cementitious material, is yielded by mixing thickened tailings (including 70–85% solid content), binder (usually 3–7% by weight) and water in a plant commonly situated at the ground surface of a mine. Thereafter, the obtained CPB mixture is transported to the underground voids created by ore extraction through pipes by pumping and/or under gravity. The recycling of tailings not only decreases the cost of constructing tailings-storage facilities, such as dams and embankments, but also reduces environmental and geotechnical threats (including acid mine drainage, water and land pollution and potential dam failure) caused by the surface disposal of tailings (Buckby *et al*., 2003). Besides its economic and environmental benefits, CPB maintains the ground stability in the mining area, which typically increases the ore recovery ratio. Moreover, some CPB structures, particularly those with a sufficient curing time, can also bear heavy equipment when exploiting the adjacent stopes (Benzaazoua *et al*., 2004). This makes mechanical stability an important property to be taken into account when CPB structures are designed.

The uniaxial compressive strength (UCS) of CPB is one of the key parameters commonly adopted to assess the mechanical properties of CPB structures. Many studies have been conducted in the past to evaluate the evolution of the UCS of CPB under varying thermal, hydraulic, mechanical and chemical conditions (Fall *et al*., 2010; Simms and Grabinsky, 2009; Yilmaz *et al*., 2009). However, the stability of CPB structures is also substantially influenced by the shear resistance at the interface between CPB and its surrounding or adjacent rocks. The assessment of this shear resistance or behaviour is essential for the determination or quantification of the arching effect (as shown in Figure 1), which can significantly reduce the vertical stress in the backfill body (in comparison with the stress caused by the self-weight of the CPB) (Marston, 1930; Pirapakaran and Sivakugan, 2007). Moreover, mine excavations advancing under sillmats (structural elements used in cut-and-fill mining of small to medium width, steeply dipping ore zones to allow extraction of ore sill pillars) must remain stable when exposed and subjected to mine-induced stresses. The sillmat is frequently made of CPB with a high binder content (De Souza and Dirige, 2002; Fang and Fall, 2018). The shear strength or shear characteristics of the sillmat–rock interface are critical data in assessing sillmat stability. Furthermore, a thorough investigation into the shear characteristics of the short- and long-term CPB–rock interfaces will lead to an improved design of a stable and more economical backfill structure. In other words, less cement will be consumed in the design of CPB structures, which will reduce the cost (75% caused by cement usage) remarkably, therefore resulting in a more cost-effective design of CPB and barricades (Grice, 2001). On the other hand, acquiring a more thorough knowledge of the interface shear performance is also critical for operation of a

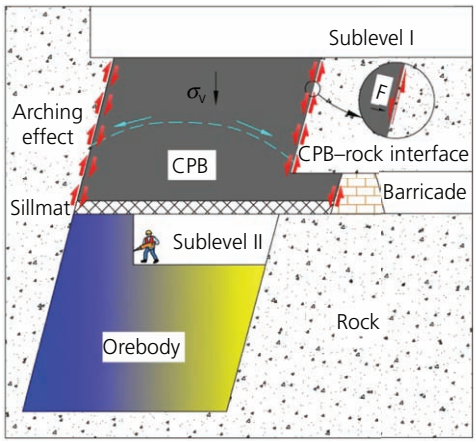

Figure 1. CPB structure and sillmat over a working area in a mine

mine in which the underhand cut-and-fill mining method with CPB is used (Figure 1). In this condition, the stability of the CPB body above the working areas and the safety of the mineworkers are influenced by the interface shear strength. The underestimation of the long-term interface shear resistance would result in the failure of the fill mass, which can have significant human (e.g. injuries, fatalities), social and financial consequences for mines (De Souza and Dirige, 2002; Pakalnis *et al*., 2005). However, there is limited research in the literature aimed at addressing the shear properties/ behaviour of the CPB–rock interface (Aubertin *et al*., 2003; Fang and Fall, 2018; Koupouli *et al*., 2016; Nasir and Fall, 2008). Despite the achievements in investigating the general shear behaviour of the interface in these studies, none of them focused on the effects of sulfate or internal sulfate attack on the long-term interface shear characteristics. For the reasons mentioned earlier as well as the fact that CPB often contains sulfate ions, there is a need to bridge the research gap. Sulfate ions are introduced into CPB structures from many sources, such as when sulfide minerals found in the tailings (a primary source of sulfate in CPB) undergo oxidation reaction or through the natural degradation of cyanides, which are usually found in gold mine processing waters. It could also come from the process of adding gypsum ($CaSO_4 \cdot 2H_2O$) for flash setting control of cement (Fall and Benzaazoua, 2005).

In response, the goal of this research is to assess experimentally the shear strength and behaviour at the CPB–rock interface cured for long durations and exposed to internal sulfate attack or effect.

Experimental process

Materials adopted

Tailings

The samples tested in this study were produced with silica tailings (STs), 99.8% of which are made up of quartz (SiO_2). Using STs helps diminish the uncertainties in the results associated with the adoption of natural tailings (NTs). Indeed, NTs contain various reactive minerals that usually oxidise during the preparation of CPB samples as well as interfere with the cement hydration mechanism, ultimately influencing the accuracy of the results (Cui and Fall, 2016; Jiang *et al*., 2017; Wang *et al*., 2016). STs are also a good substitute to use in place of NTs because they have a particle size distribution comparable with that of the tailings produced in Canadian mines, as shown in Figure 2.

Binder

Portland cement type I (PCI) was utilised to produce the CPB components of the samples. PCI is the prevalent binder material used in CPB operations.

Mixing water

CPB samples with varying sulfate contents had to be prepared. A specific amount of iron (II) sulfate heptahydrate ($FeSO_4 \cdot 7H_2O$) was dissolved in distilled water to produce solutions with sulfate concentrations of 0, 5000, 15 000 and 25 000 parts per million (ppm).

Rock samples

Granite (with dimensions of 60 × 60 × 10 mm) was polished to work as the rock base. This polishing creates a rock surface of similar roughness, so that the effect of the sulfate on the CPB–rock interface can be assessed with a high degree of accuracy – that is, the shear behaviour of the interface will not be affected by uncertainties due to the use of rocks with slightly different surface roughness. The joint roughness coefficient was used to evaluate the shear strength through comparisons with typical roughness profiles, and according to Tse and Cruden (1979), the surface roughness of granite is zero.

Specimen preparation and testing procedure

Specimen preparation

A food mixer was used to produce the CPB mixture. After thoroughly mixing specific amounts of STs, PCI (4.5%) and water with various sulfate contents for 7 min (a common mixing time in practice), the obtained homogeneous paste (with a water/cement

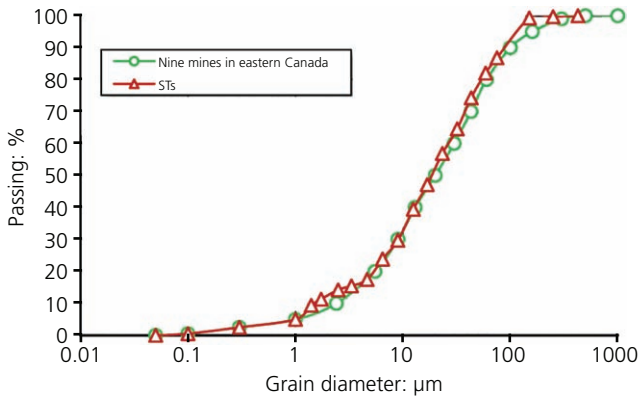

Figure 2. Comparison of the particle size distribution of STs and the average particle size distribution of NTs from nine Canadian mines

(w/c) ratio of 7.35 and a solid content of 76%) was then poured into square plastic containers with the granite. The container dimensions are 60 × 60 × 30 mm, matching the size of the direct shear box. Thereafter, the entire sample was subjected to manual vibration to ensure that there was no air trapped in the CPB. After removing the air, the containers were then covered with plastic film and allowed to cure at a temperature of 20°C until testing at different times. Figure 3 shows specimens of CPB containing different initial sulfate contents cast on rock surfaces and cured for 150 days.

Testing procedure

After the samples with varying initial sulfate contents were cured for 28, 90 and 150 days, direct shear tests were carried out under three constant normal stresses (50, 100, 150 kPa). These normal stresses can represent the horizontal (normal) stresses applied at the interface between the rock mass and a backfill structure up to 40 m high, considering the arching effect. Figure 4 shows the experimental scheme. As shown in the figure, each node refers to an experimental condition – for example, the red node corresponds to the following condition: a 100 kPa normal stress applied onto a 5000 ppm sample that was cured for 90 days. The nodes in the blue plane represent samples that were cured for 150 days. For accuracy, the testing for each sample was performed at least three times. Therefore, more than 108 sets of direct shear tests were conducted in this study.

Mechanical tests and microstructural analyses

Direct shear testing

In compliance with the ASTM D 3080-04 standard (ASTM, 2004), direct shear tests on interface samples were performed at a loading rate of 0.5 mm/min. The experimental results, including the horizontal and normal displacements, as well as the shear stress, were collected through the LabView computer application.

Microstructural analyses

Different microstructural tests were conducted to assess the influence of sulfate on the evolution of the pore structure and the amount of hydration products in CPB. They include thermogravimetric (TG) analysis, differential TG (DTG) test, X-ray diffraction (XRD) and mercury (Hg) intrusion porosimetry (MIP). The thermal analyses were conducted on oven-dried (temperature of 40–45°C for at least 4 days) cement paste powder (with w/c of 2) using a Q5000 IR TG analyser. The TG and DTG

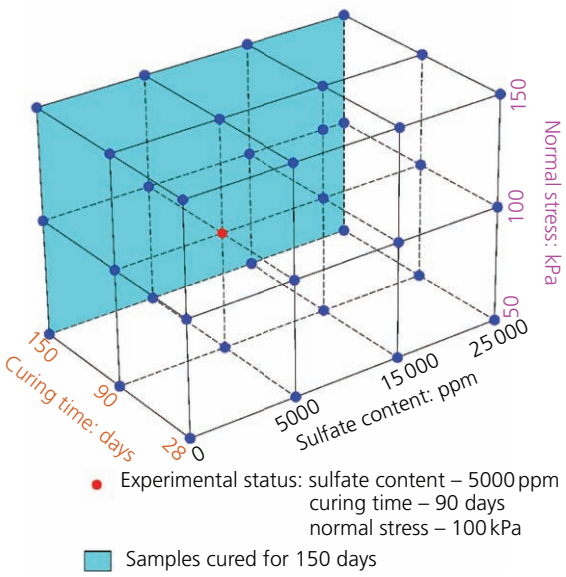

Figure 4. Experimental scheme

results were used to assess the progress of hydration in the cement paste with different sulfate contents. XRD was also performed on the cement paste powder using a Scintag XDS-2000 diffractometer, and its results were used to determine the mineralogical composition of the samples with different ages and various sulfate contents. The MIP test was performed on the oven-dried CPB samples (with a temperature between 40 and 45°C for at least 4 days) using a Micromeritics AutoPore III-9420 mercury porosimeter, and using the results, the porosity of differently sulfated CPB samples can then be analysed.

Results and explanation

Effects of sulfate ions on interface shear behaviour

Figure 5 presents plots of shear displacement against shear stress of the interface between granite and CPB samples with varying initial sulfate contents that were cured for 28, 90 and 150 days. The plots show that the shear stress curves exhibit similar trends and shapes, increasing steadily up to the shear strength followed by a sudden failure (in bonding), irrespective of the curing time and the sulfate content. The sudden bond failure is due to the weakening of the

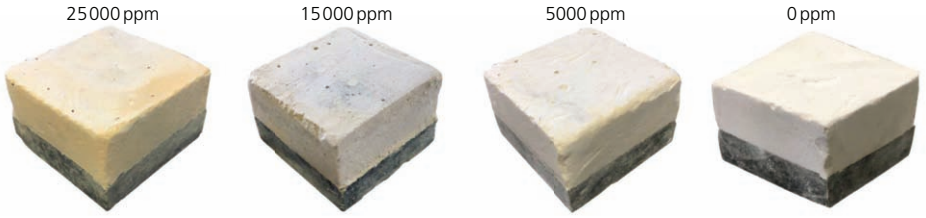

Figure 3. Interface of samples with various initial sulfate contents (150 days)

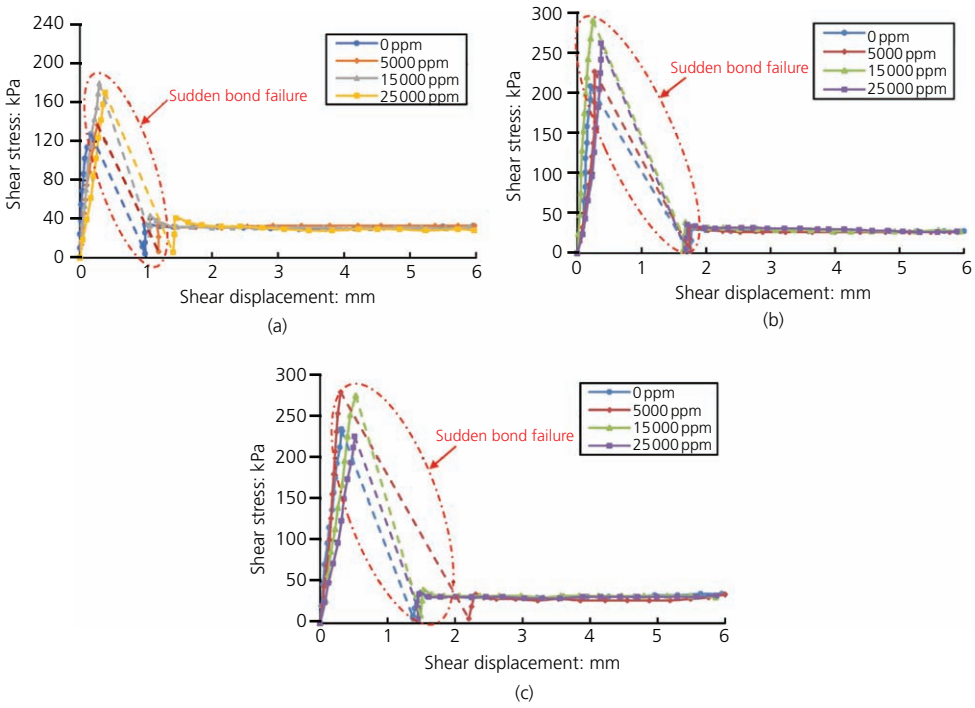

Figure 5. Shear displacement–shear stress curves of interface samples (normal stress: 50 kPa): (a) 28 days of curing; (b) 90 days of curing; (c) 150 days of curing

hardened cement that bonds the CPB to the rock surface (interface bonding failure) at a low normal stress (Saiang *et al*., 2005; Seidel and Haberfield, 2002; Swedenborg, 2003; Tian *et al*., 2015). Meanwhile, it is noticeable that the interface peak shear stress (shear strength) is dependent not only on the curing time but also on the initial sulfate content, as discussed below.

Figure 6 is a plot of the shear behaviour (shear displacement against normal displacement) of the aforementioned interfaces with varying sulfate contents and curing times. It shows that for all the samples, the interface undergoes a slight contraction during the beginning of the direct shear tests. These contractions are caused by the inherent compressibility of the CPB samples. Such contraction behaviour was observed previously by Nasir and Fall (2008). Thereafter, the interfaces of all of the samples show obvious dilation until bonding failure at the interface. Beyond the point that corresponds to this bonding failure, the samples then generally showed continuous contracting behaviour.

It can also be inferred from Figure 6 that the sulfate content does not have a significant effect on the interface contraction behaviour. However, the amount of shear dilation is impacted by the curing time and the initial sulfate concentration, which is presented in Figure 7. The figure indicates the amount of maximum shear dilation of the interface with variable sulfate contents at different curing times. Notably, Figures 6 and 7 reveal that the value of the maximum shear dilation increases gradually as the curing time extends (with the exception of the 25 000 ppm samples that were cured for 150 days). This rise in shear dilation with curing time is caused by the intensification of cement hydration with time (Husem and Gozutok, 2005), which generates stronger asperities at the surface (Hou *et al*., 2019; Nasir and Fall, 2008). Stronger asperities are more resistant to damage during the shearing or the sliding of the surface at the interface. Consequently, the interface of the samples with a longer curing time shows more dilation. However, Figures 6 and 7 indicate that although there are no significant differences (in considering the experimental errors associated with these tests) in the maximum shear dilation values of the 90-day samples, the maximum shear dilation value of the 25 000 ppm samples are significantly lower than those of the 0, 5000 and 15 000 ppm samples after being cured for 150 days. This lower dilation of the 25 000 samples is attributed to the high sulfate content, which weakens the asperities at the surface of the CPB, thereby leading to lower shear dilation of the interface. The negative contribution of a high sulfate content to the shear strength has been linked to the influences through four processes: (*a*) the retardation of cement hydration by sulfate, (*b*) the generation of expansive hydration products (particularly ettringite), (*c*) the coarser capillary structure in CPB and (*d*) the adsorption of sulfate molecules by calcium silicate hydrates (C-S-H).

Contribution of sulfate ions to the interface shear strength evolution

Figure 8 shows the change in shear strength against time and sulfate concentration at the interface. The results show that sulfate

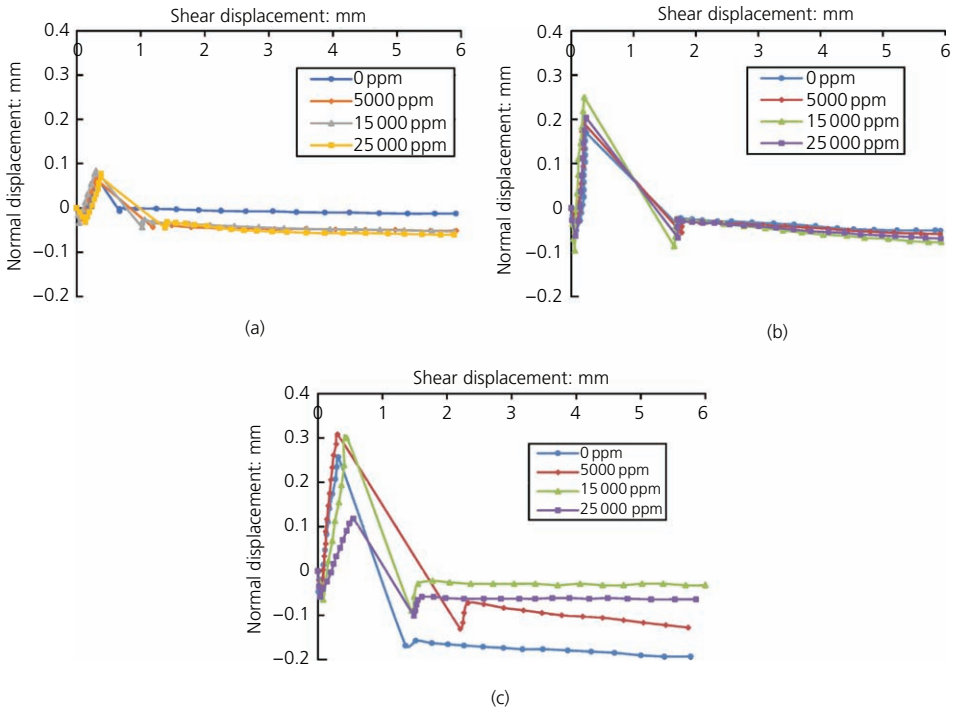

Figure 6. Shear displacement–vertical displacement curves of interface samples (normal stress: 50 kPa): (a) 28 days of curing time; (b) 90 days of curing time; (c) 150 days of curing time

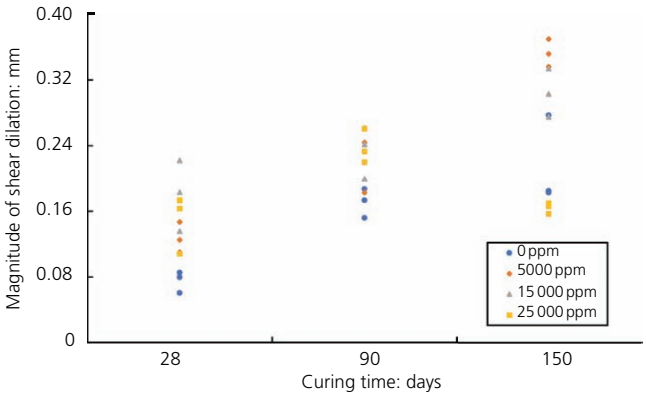

Figure 7. Changes in shear dilation values at the interface (normal stress: 50 kPa)

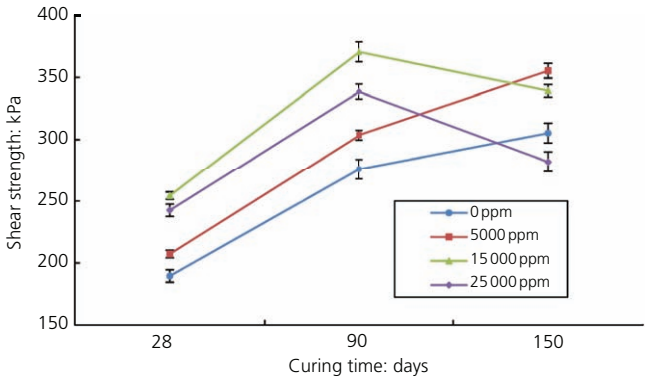

Figure 8. Changes in interface shear strength (normal stress: 150 kPa)

exerts considerable effects on the interface shear strength. Moreover, it is observable that the extent of the contributions of sulfate on the shear strength evolution is a function of the curing time, as discussed below.

Prior to the further discussion of the observed changes in the shear strength under different sulfate contents, it is important to recall the following key factors that impact the mechanical strength of CPB or any cementitious material. (*a*) The first is the amount of C-S-H produced, because C-S-H is the principal binding element in a hardened cemented system (Gan, 1997). Therefore, greater cement hydration means that there is more C-S-H (Fall *et al*., 2010). However, C-S-H adsorbs sulfate to form weaker C-S-H gel (characterised with a weaker intrinsic mechanical strength), consequently reducing the strength of the cementitious materials (e.g. CPB) (Bentur, 1976; Jelenić *et al*., 1977; Pelisser *et al*., 2012). It is well known that the sulfate adsorption by C-S-H is also influenced by the amount of sulfate available. A high sulfate content means an increased rate of adsorption (Fu *et al*., 1997; Ramlochan *et al*., 2003). (*b*) The second factor is the quantity of expansive minerals (mainly ettringite and gypsum) that are produced in the CPB system due

to the presence of sulfate ions, considering that gypsum and ettringite are products of reactions between sulfate ions and calcium hydroxide ($Ca(OH)_2$; hereafter 'CH') and tricalcium aluminate ($3CaO{\cdot}Al_2O_3$), respectively (Husem and Gozutok, 2005; Li and Fall, 2016). The presence of expansive minerals can influence the mechanical strength of CPB either negatively or positively depending on the amount of the stated expansive minerals and the size of the capillary pores (Li and Fall, 2016, 2018). On the one hand, the precipitation of sufficient (rather than excessive) amounts of expansive minerals inside the CPB tends to refine the capillary structure, ultimately contributing to an improvement of the CPB mechanical strength (Pokharel and Fall, 2013). In contrast, the excessive formation of expansive minerals causes physical damage and brings about the development of a larger pore structure in the CPB, thereby decreasing its mechanical strength (Fall and Pokharel, 2010).

Twenty-eight days of curing

As indicated in Figures 5 and 8, the shear strength of 28-day samples containing sulfate is stronger than that of the ones without sulfate. Moreover, the shear strength grows as the sulfate content rises, except for the 25 000 ppm samples.

This higher shear strength and the increase along with the sulfate content (rising up to 15 000 ppm) are due to the refinement of the CPB structure as a result of the deposition of gypsum and ettringite as discussed above. This refinement of the CPB pores increases the contact area of CPB with the rock, leading to a harder interlocking structure at the interface of the sulfate-bearing samples (Fang and Fall, 2019). The argument concerning pore refinement caused by the deposition of more expansive materials in CPB with sulfate is evident from the outcomes of scanning electron microscopy (SEM) conducted on CPB samples that contain sulfate (Fall *et al*., 2005), as well as by those of MIP analyses performed on 0 and 5000 ppm samples, as presented in Figure 9. The SEM observations of the 28-day-cured samples by Fall *et al*. (2005) revealed that the pores in the paste backfill containing sulfate are mainly filled up by secondary gypsum. Figure 9 clearly shows that compared with the pore structure of the 0 ppm sample, the 5000 ppm sample considerably has a finer capillary structure. Moreover, the 5000 ppm samples contain more expansive minerals (in comparison with the sulfate-free sample), which is attested by the thermal analysis results shown in Figure 10. Generally, the weight loss situated at 30–105°C on the DTG curve is the result of water evaporation, while the peak occurring from 110 to 170°C is attributed to the desiccation of some hydration products, mainly including C-S-H, gypsum and ettringite (Fang *et al*., 2021; Nonnet *et al*., 1999). The higher weight loss of the 5000 ppm samples at a temperature of 110–170°C (compared with samples without sulfate) suggests that there are more expansive minerals. The aforementioned lower strength associated with the 25 000 ppm samples (compared with the 15 000 ppm samples) is caused by the following two processes: (*a*) the sulfate-induced retardation of cement hydration (Fall and Pokharel, 2010; Tzouvalas *et al*., 2004), which results in the generation of less C-S-H, and (*b*) the pronounced adsorption of sulfate by C-S-H at high sulfate contents, which produces weaker C-S-H gel (Jelenić *et al*., 1977; Tian and Cohen, 2000). Consequently, the less C-S-H and weaker C-S-H gel result in a weaker adhesion between the CPB and rock with the sulfate content being raised to 25 000 ppm. This generates weaker asperities and binding forces at the interface, thereby decreasing the shear strength. The retardation of the cement hydration by sulfate is proven by the outcomes of the thermal analyses carried out on 0, 5000 and 25 000 ppm samples (see Figure 10). The TG and DTG curves of the samples with various initial sulfate concentrations show that there is less weight loss when the temperature falls in the range 400–450°C (due to CH decomposition (Haiqiang *et al*., 2016; Pane and Hansen, 2005)) as the sulfate content increases. Less CH, particularly in the 25 000 ppm samples, corresponds to a lower level of cement hydration and thus a smaller quantity of C-S-H.

It is also noticeable from Figure 8 that despite the aforementioned inhibition effect, the observed shear strength of the 25 000 ppm samples is still higher than those of the 0 and 5000 ppm samples. This observation suggests that there is a competition between the

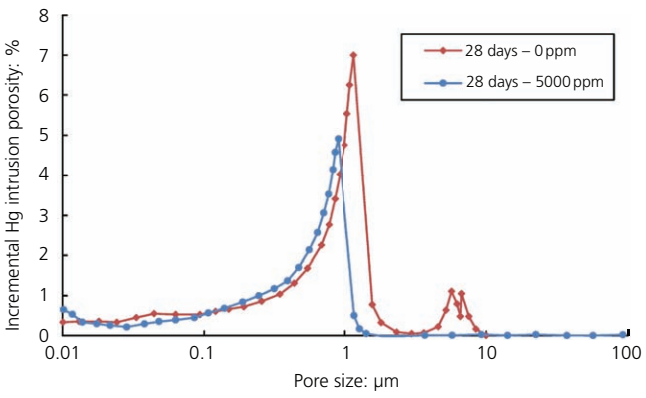

Figure 9. Pore size distribution of 0 and 5000 ppm samples

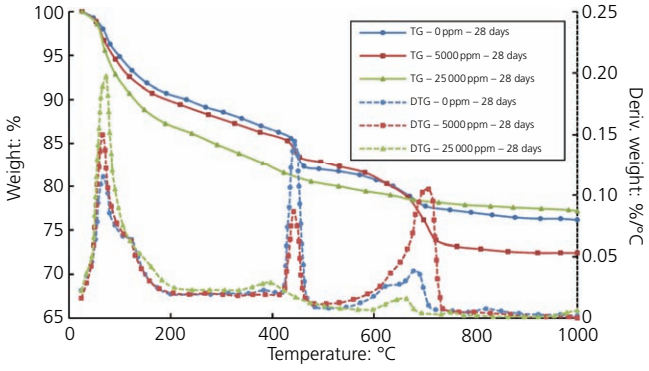

Figure 10. TG and DTG diagrams of differently sulfated samples

processes of shear strength development (due to the capillary structure refinement by expansive minerals) and shear strength reduction (the retardation of binder hydration) when the sulfate content in CPB rises.

Ninety days of curing

Figure 8 indicates that after 90 days of curing, the interface of all of the samples shows growth in shear strength, irrespective of the sulfate concentration. The growth in the shear strength with curing time is caused by the ongoing cement hydration. In fact, with the increasing curing time, CPB tends to become harder because of the continued hydration of the binder. The hardening process induces the generation of stronger asperities at the interface, thereby increasing the critical stress value required for the breaking of these asperities (Fall and Nasir, 2010). This obviously means that a higher shear stress will be required for the bonding failure of the cement. Furthermore, it is also noticeable from Figure 8 that the strength of 90-day samples shows the same order as those with a curing length of 28 days. In other words, the shear strength of the most highly sulfated samples is lower than that of the 15 000 ppm interface but higher than that of the 5000 ppm samples. The reasons for this phenomenon are the same as those provided for the 28-day samples.

One hundred and fifty days of curing

Figure 8 shows that the shear strength of the 0 and 5000 ppm samples continues to increase while the curing age extends from 90 to 150 days. The interpretations for this behaviour have already been discussed earlier.

In contrast, the 15 000 and 25 000 ppm samples show a significant reduction in shear strength. Moreover, the decreasing rate of the former is less than that of the 25 000 ppm sample. This observably significant drop in the shear strength of highly sulfated samples and the higher decreasing rate of 25 000 ppm samples are due to the combined effects of the three processes: (*a*) formation of excessive amounts (in terms of the size of the capillary pores) of expansive minerals, particularly gypsum (Equation I); (*b*) retardation of the binder hydration; and (*c*) sulfate adsorption by C-S-H.

$$\text{I.}\quad SO_4^{2-} + Ca(OH)_2 + 2H_2O \rightarrow CaSO_4 \cdot 2H_2O + 2OH^- \tag{I}$$

The precipitation of a large quantity of gypsum in the capillary pores means that excessive pressure will be generated inside the pores of CPB (Ping and Beaudoin, 1992). This pressure, which is higher with more sulfate, results in physical damages (e.g. generation of microcracks) inside the CPB matrix. Specifically, the excessive pressure will weaken the asperities at the interface and reduce the cementation binding force. Subsequently, the shear strength of the higher-sulfate-content samples is reduced. The sulfate-induced physical damages or development of a larger pore structure in CPB with high sulfate concentrations is confirmed by the outcomes of the SEM and MIP tests reached in the study by Aldhafeeri and Fall (2017) and Figure 11, respectively. The SEM observation of the 150-day CPB sample with 25 000 ppm sulfate content illustrates the formation of many cracks inside the CPB. Figure 11, which illustrates the outcomes of the MIP tests carried out on 150-day CPB samples, shows that the most highly sulfated specimen has a less dense pore structure than the sulfate-free specimen.

Moreover, the aforementioned retardation of the binder hydration in the samples with a large volume of sulfate contributes to the generation of fewer hydration products (particularly C-S-H), which eventually leads to a reduced interface peak shear stress. C-S-H is the key contributor to the strength growth of any Portland-cement-based materials (Gan, 1997). Induced by sulfate, this inhibition of the binder hydration concurs with the outcomes reached by the XRD analyses targeted at the 150-day samples with relatively low (5000 ppm) and high (25 000 ppm) sulfate contents, as presented in Figure 12. It is clearly noticed that the 25 000 ppm specimen still includes unreacted bicalcium silicate (C_2S) and tricalcium silicate (C_3S) even after being cured for 150 days, whereas none of these minerals is observed within the sample with a 5000 ppm sulfate content, indicating that the former has not fully hydrated or its degree of hydration is lower than that of the latter.

Furthermore, the generation of C-S-H gel, which is generated by the reaction between C-S-H and extra sulfate ions, reduces the interface strength (Fang and Fall, 2019; Jelenić *et al.*, 1977). It is particularly obvious when it comes to highly sulfated samples. This phenomenon is also documented by studies conducted by other researchers (Barbarulo, 2002; Divet and Randriambololona, 1998).

A closer look at the shear strength values of the 150-day samples presented in Figure 8 also reveals that the 5000 ppm sample is credited with the strongest peak shear stress. This is a result of the following mechanisms: (*a*) the refinement of the pore structure of the 5000 ppm CPB owing to the deposition of sufficient gypsum, as discussed previously and demonstrated in numerous previous studies

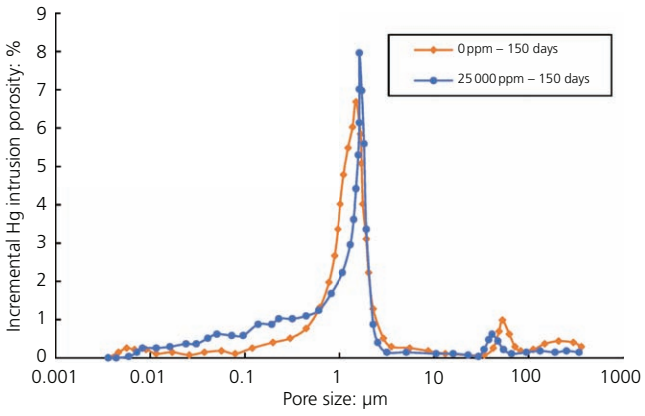

Figure 11. Pore size distribution of 0 and 25 000 ppm samples (150 days)

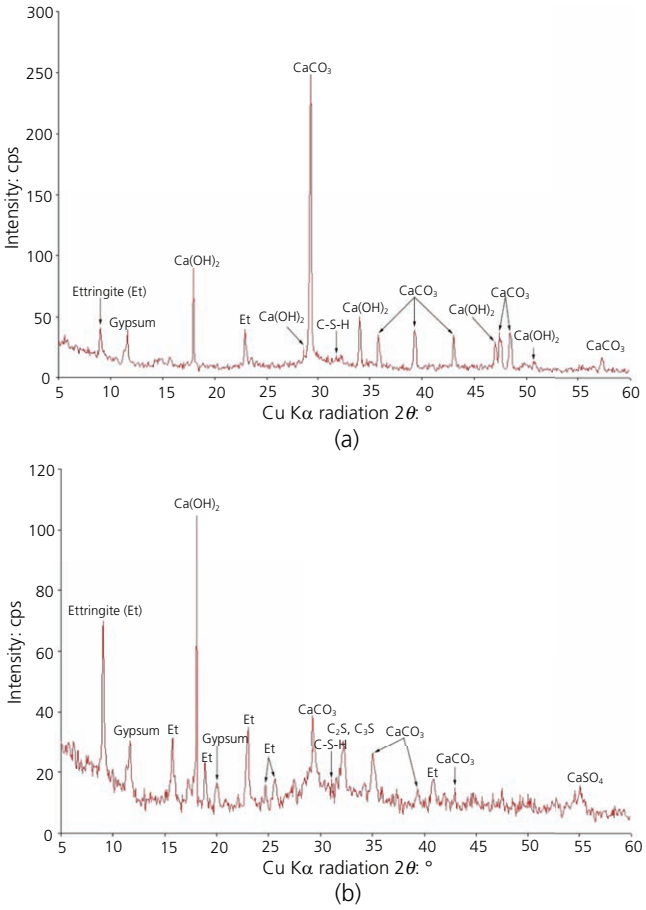

Figure 12. XRD results of cement paste with a curing time of 150 days: (a) 5000 ppm; (b) 25 000 ppm. cps, counts per second; C_2S, bicalcium silicate; C_3S, tricalcium silicate

(Fall *et al*., 2005), and (*b*) the insignificant inhibition of the binder hydration in samples with a 5000 ppm sulfate content. The absent or low inhibition effect is in agreement with the XRD analyses presented in Figure 12. It can be noticed that there are no unreacted C_2S and C_3S in the 5000 ppm samples, while the samples with 25 000 ppm of sulfate show unreacted C_2S and C_3S. These observations indicate that, similar to the samples with curing times of 28 and 90 days, there is also a competition between the processes that contribute to an increase in strength (generation of a larger amount of cement hydration products) and a decrease in strength (sulfate-induced retardation of the binder hydration, formation of C-S-H gel, coarsening and microcracking of the CPB matrix). To put it in another way, the dominant factors that affect the strength evolution (reducing or increasing) of the samples in this study are the initial sulfate content and the curing time.

Contribution of sulfate ions to the evolution of the interface shear strength parameters

An analysis of the data obtained showed that the Mohr–Coulomb failure criterion can be utilised to establish the shear failure envelope

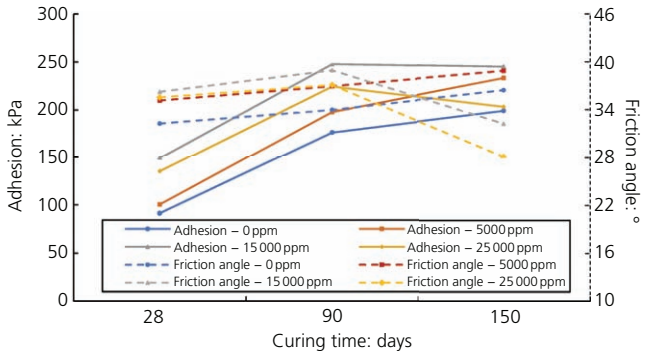

Figure 13. Development of CPB–rock interface shear strength parameters

of the specimens. Thereafter, the shear strength parameters can be deduced based on the Mohr–Coulomb failure criterion. Figure 13, which shows the time- and sulfate-dependent variations in the shear strength parameters, indicates that the evolutions of the interface friction angle and adhesion are significantly associated with the curing age and initial sulfate concentration. In detail, both the friction angle and the adhesion of 0 and 5000 ppm samples increase with curing age. The finding also agrees with the outcomes achieved by previous studies concerning the CPB–rock interface and cemented soils (Koupouli *et al*., 2016; Uddin *et al*., 1997). The increased adhesion is generated by the increase in binding force at the interface owing to the enhanced cement hydration (Nasir and Fall, 2008). On the other hand, the slight increase in friction angle is attributed to stronger asperities formed at the interface. The stronger asperities that form interlocking structures at the interface are cemented together by the multiplying binder hydration products with curing time (Lade and Overton, 1989). This in turn results in a higher frictional resistance at the interface, thus increasing the friction angle.

However, for 15 000 and 25 000 ppm samples, the adhesion and friction angle show an increase during the first 90 days but then experience a gradual decrease from 90 to 150 days. The processes that are responsible for this reduction in adhesion and friction angle are the same as those accounting for the aforementioned decline concerning the shear strength of these highly sulfated samples. Specifically, the excessive pressure applied by profuse expansive minerals in the pores leads to physical destruction to the microstructure of the bonding phase at the interface, thereby reducing the adhesion. The generation of a smaller amount of C-S-H (due to sulfate-induced inhibition) and lower-quality C-S-H gel (due to sulfate adsorption) are additional factors that contribute to reduced adhesion at the interface.

Conclusions

The experimental results of the effect of the initial sulfate concentration on the shear performance of the CPB–rock interface samples at advanced ages are presented in this paper. The main conclusions are summarised as follows.

- Sulfate ions considerably affect the interface shear characteristics, and the effect varies with the initial sulfate concentration and curing time. The changes in the initial sulfate concentration and the curing time can have positive or negative effects on the long-term shear strength of the CPB–rock interface.
- The processes that increase the shear strength include (*a*) the generation of a larger amount of C-S-H with time and (*b*) the refinement of the capillary structure of CPB owing to the deposition of sufficient amounts of gypsum and ettringite. The combined effect of these processes leads to stronger binding force and a larger contacting area at the interface, thereby resulting in the formation of stronger asperities at the interface.
- For 15 000 and 25 000 ppm samples, the processes that account for the decreasing shear strength are (*a*) the more significant retardation effect on the cement hydration with increasing sulfate concentration; (*b*) the production of an excessive quantity of gypsum, which leads to physical damage to the microstructure; and (*c*) the generation of lower-quality C-S-H gel.
- It is found that there is a competition between the processes that increase or reduce the shear strength. The extent of the effect is related to the initial sulfate concentration and the curing ages.

The outcomes of this study allow a more in-depth understanding and evaluation of the CPB–rock interface shear performance, which is critical for building cost-effective backfill structures. Despite the results obtained, it should be pointed out that the impact of factors such as the scale effect, the influence of interface roughness, normal stresses and CPBs consisting of different binders (ordinary Portland cement (OPC)–slag, OPC–fly ash) was not considered in this research. It would be interesting to address this gap in future studies.

Acknowledgements

The Natural Sciences and Engineering Research Council of Canada and the China Scholarship Council are appreciated for the funding. The authors also extend their appreciation to Mr Jean Claude Celestin and Dr Jiwei Bian for their kind help.

REFERENCES

Aldhafeeri Z and Fall M (2017) Sulphate induced changes in the reactivity of cemented tailings backfill. *International Journal of Mineral Processing* **166**: 13–23, https://doi.org/10.1016/j.minpro.2017.06.007.

Amaratunga L and Yaschyshyn D (1997) Development of a high modulus paste fill using fine gold mill tailings. *Geotechnical & Geological Engineering* **15(3)**: 205–219.

ASTM (2004) D 3080-04: Standard test method for direct shear test of soils under consolidated drained conditions. ASTM International, West Conshohocken, PA, USA.

Aubertin M, Li L, Arnoldi S *et al.* (2003) Interaction between backfill and rock mass in narrow stopes. In *Soil and Rock America 2003: Proceedings of 12th Panamerican Conference on Soil Mechanics and Geotechnical Engineering and 39th U.S. Rock Mechanics Symposium* (Culligan PJ, Einstein HH and Whittle AJ (eds)). Verlag Glückauf, Essen, Germany, vol. 1, pp. 1157–1164.

Barbarulo R (2002) *Comportement des Matériaux Cimentaires: Actions des Sulfates et de la Température*. PhD thesis, Ecolé Normale Supérieure de Cachan, Cachan, France (in French).

Bentur A (1976) Effect of gypsum on the hydration and strength of C3S pastes. *Journal of the American Ceramic Society* **59(5–6)**: 210–213, https://doi.org/10.1111/j.1151-2916.1976.tb10935.x.

Benzaazoua M, Fall M and Belem T (2004) A contribution to understanding the hardening process of cemented pastefill. *Minerals Engineering* **17(2)**: 141–152, https://doi.org/10.1016/j.mineng.2003.10.022.

Brackebusch F (1995) Basics of paste backfill systems. *International Journal of Rock Mechanics & Mining Sciences and Geomechanics Abstracts* **32(3)**: 122A, https://doi.org/10.1016/0148-9062(95)90153-V.

Buckby T, Black S, Coleman ML and Hodson M (2003) Fe-sulphate-rich evaporative mineral precipitates from the Rio Tinto, southwest Spain. *Mineralogical Magazine* **67(2)**: 263–278, https://doi.org/10.1180/0026461036720104.

Cui L and Fall M (2016) Mechanical and thermal properties of cemented tailings materials at early ages: influence of initial temperature, curing stress and drainage conditions. *Construction and Building Materials* **125**: 553–563, https://doi.org/10.1016/j.conbuildmat.2016.08.080.

De Souza E and Dirige AP (2002) An integrated approach for the design of stable mine backfill sillmats. In *Damage and Fracture Mechanics VII: Computer Aided Assessment and Control* (Brebbia CA and Nishida SI (eds)). WIT Press, Southampton, UK, pp. 303–312.

Divet L and Randriambololona R (1998) Delayed ettringite formation: the effect of temperature and basicity on the interaction of sulphate and CSH phase. *Cement and Concrete Research* **28(3)**: 357–363, https://doi.org/10.1016/S0008-8846(98)00006-4.

Fall M and Benzaazoua M (2005) Modeling the effect of sulphate on strength development of paste backfill and binder mixture optimization. *Cement and Concrete Research* **35(2)**: 301–314, https://doi.org/10.1016/j.cemconres.2004.05.020.

Fall M and Nasir O (2010) Mechanical behaviour of the interface between cemented tailings backfill and retaining structures under shear loads. *Geotechnical and Geological Engineering* **28(6)**: 779–790.

Fall M and Pokharel M (2010) Coupled effects of sulphate and temperature on the strength development of cemented tailings backfills: Portland cement-paste backfill. *Cement and Concrete Composites* **32(10)**: 819–828, https://doi.org/10.1016/j.cemconcomp.2010.08.002.

Fall M, Benzaazoua M and Ouellet S (2005) Experimental characterization of the influence of tailings fineness and density on the quality of cemented paste backfill. *Minerals Engineering* **18(1)**: 41–44, https://doi.org/10.1016/j.mineng.2004.05.012.

Fall M, Célestin J, Pokharel M and Touré M (2010) A contribution to understanding the effects of curing temperature on the mechanical properties of mine cemented tailings backfill. *Engineering Geology* **114(3–4)**: 397–413, https://doi.org/10.1016/j.enggeo.2010.05.016.

Fang K and Fall M (2018) Effects of curing temperature on shear behaviour of cemented paste backfill–rock interface. *International Journal of Rock Mechanics and Mining Sciences* **112**: 184–192, https://doi.org/10.1016/j.ijrmms.2018.10.024.

Fang K and Fall M (2019) Chemically induced changes in the shear behaviour of interface between rock and tailings backfill undergoing cementation. *Rock Mechanics and Rock Engineering* **52(9)**: 3047–3062.

Fang K, Ren L and Jiang H (2021) Development of mode I and mode II fracture toughness of cemented paste backfill: experimental results of the effect of mix proportion, temperature and chemistry of the pore water. *Engineering Fracture Mechanics* **258**: article 108096, https://doi.org/10.1016/j.engfracmech.2021.108096.

Fu Y, Ding J and Beaudoin J (1997) Expansion of Portland cement mortar due to internal sulfate attack. *Cement and Concrete Research* **27(9)**: 1299–1306, https://doi.org/10.1016/S0008-8846(97)00133-6.

Gan M (1997) *Cement and Concrete*. CRC Press, Boca Raton, FL, USA.

Grice AG (2001) Recent mine fill developments in Australia. *Proceedings of the 7th International Symposium on Mining with Backfill: Minefill, Seattle, WA, USA*, pp. 351–357.

Haiqiang J, Fall M and Cui L (2016) Yield stress of cemented paste backfill in sub-zero environments: experimental results. *Minerals Engineering* **92**: 141–150, https://doi.org/10.1016/j.mineng.2016.03.014.

Hassani F and Archibald J (eds) (1998) *Mine Backfill 1998*. Canadian Institute of Mining, Metallurgy and Petroleum, Montreal, QC, Canada.

Hou C, Zhu W, Yan B, Guan K and Niu L (2019) Analytical and experimental study of cemented backfill and pillar interactions. *International Journal of Geomechanics* **19**: article 04019080.

Husem M and Gozutok S (2005) The effects of low temperature curing on the compressive strength of ordinary and high performance concrete. *Construction and Building Materials* **19(1)**: 49–53, https://doi.org/10.1016/j.conbuildmat.2004.04.033.

Jelenić I, Panović A, Halle R and Gaćeša T (1977) Effect of gypsum on the hydration and strength development of commercial Portland cements containing alkali sulfates. *Cement and Concrete Research* **7(2)**: 239–245, https://doi.org/10.1016/0008-8846(77)90085-0.

Jiang HFall MCui L (2017) Freezing behaviour of cemented paste backfill material in column experiments. *Construction and Building Materials* **147**: 837–846, https://doi.org/10.1016/j.conbuildmat.2017.05.002.

Koupouli NJ, Belem T, Rivard P and Effenguet H (2016) Direct shear tests on cemented paste backfill–rock wall and cemented paste backfill–backfill interfaces. *Journal of Rock Mechanics and Geotechnical Engineering* **8(4)**: 472–479, https://doi.org/10.1016/j.jrmge.2016.02.001.

Lade PV and Overton DD (1989) Cementation effects in frictional materials. *Journal of Geotechnical Engineering* **115(10)**: 1373–1387.

Li WC and Fall M (2016) Sulphate effect on the early age strength and self-desiccation of cemented paste backfill. *Construction and Building Materials* **106**: 296–304, https://doi.org/10.1016/j.conbuildmat.2015.12.124.

Li WC and Fall M (2018) Strength and self-desiccation of slag-cemented paste backfill at early ages: link to initial sulphate concentration. *Cement and Concrete Composites* **89**: 160–168, https://doi.org/10.1016/j.cemconcomp.2017.09.019.

Marston A (1930) The theory of external loads on closed conduits in the light of the latest experiments. *Proceedings of the Ninth Annual Meeting of the Highway Research Board, Washington, DC, USA*, vol. 9, pp. 138–170.

Nasir O and Fall M (2008) Shear behaviour of cemented pastefill–rock interfaces. *Engineering Geology* **101(3–4)**: 146–153, https://doi.org/10.1016/j.enggeo.2008.04.010.

Nonnet E, Lequeux N and Boch P (1999) Elastic properties of high alumina cement castables from room temperature to 1600°C. *Journal of the European Ceramic Society* **19(8)**: 1575–1583, https://doi.org/10.1016/S0955-2219(98)00255-6.

Pakalnis R, Caceres C, Clapp K *et al.* (2005) Design spans – underhand cut and fill mining. *107th Canadian Institute of Mining, Metallurgy and Petroleum Annual General Meeting, Toronto, ON, Canada.*

Pane I and Hansen W (2005) Investigation of blended cement hydration by isothermal calorimetry and thermal analysis. *Cement and Concrete Research* **35(6)**: 1155–1164, https://doi.org/10.1016/j.cemconres.2004.10.027.

Pelisser F, Gleize PJP and Mikowski A (2012) Effect of the Ca/Si molar ratio on the micro/nanomechanical properties of synthetic CSH measured by nanoindentation. *Journal of Physical Chemistry C* **116(32)**: 17219–17227, https://doi.org/10.1021/jp302240c.

Ping X and Beaudoin JJ (1992) Mechanism of sulphate expansion I. Thermodynamic principle of crystallization pressure. *Cement and Concrete Research* **22(4)**: 631–640, https://doi.org/10.1016/0008-8846(92)90015-N.

Pirapakaran K and Sivakugan N (2007) A laboratory model to study arching within a hydraulic fill stope. *Geotechnical Testing Journal* **30(6)**: 496–503, https://doi.org/10.1520/GTJ100653.

Pokharel M and Fall M (2013) Combined influence of sulphate and temperature on the saturated hydraulic conductivity of hardened cemented paste backfill. *Cement and Concrete Composites* **38**: 21–28, https://doi.org/10.1016/j.cemconcomp.2013.03.015.

Ramlochan T, Zacarias P, Thomas M and Hooton R (2003) The effect of pozzolans and slag on the expansion of mortars cured at elevated temperature: part I: expansive behaviour. *Cement and Concrete Research* **33(6)**: 807–814, https://doi.org/10.1016/S0008-8846(02)01066-9.

Saiang D, Malmgren L and Nordlund E (2005) Laboratory tests on shotcrete–rock joints in direct shear, tension and compression. *Rock Mechanics and Rock Engineering* **38(4)**: 275–297.

Seidel JP and Haberfield CM (2002) A theoretical model for rock joints subjected to constant normal stiffness direct shear. *International Journal of Rock Mechanics and Mining Sciences* **39(5)**: 539–553, https://doi.org/10.1016/S1365-1609(02)00056-4.

Simms P and Grabinsky M (2009) Direct measurement of matric suction in triaxial tests on early-age cemented paste backfill. *Canadian Geotechnical Journal* **46(1)**: 93–101, https://doi.org/10.1139/T08-098.

Swedenborg S (2003) *Rock Mechanical Effects of Cement Grouting in Hard Rock*. PhD thesis, Chalmers University of Technology, Gothenburg, Sweden.

Tian B and Cohen MD (2000) Does gypsum formation during sulfate attack on concrete lead to expansion? *Cement and Concrete Research* **30(1)**: 117–123, https://doi.org/10.1016/S0008-8846(99)00211-2.

Tian H, Chen W, Yang D and Yang J (2015) Experimental and numerical analysis of the shear behaviour of cemented concrete–rock joints. *Rock Mechanics and Rock Engineering* **48(1)**: 213–222.

Tse R and Cruden DM (1979) Estimating joint roughness coefficients. *International Journal of Rock Mechanics and Mining Sciences & Geomechanics Abstracts* **16(5)**: 303–307, https://doi.org/10.1016/0148-9062(79)90241-9.

Tzouvalas G, Dermatas N and Tsimas S (2004) Alternative calcium sulfate-bearing materials as cement retarders: part I. Anhydrite. *Cement and Concrete Research* **34(11)**: 2113–2118, https://doi.org/10.1016/j.cemconres.2004.03.020.

Uddin K, Balasubramaniam A and Bergado D (1997) Engineering behavior of cement-treated Bangkok soft clay. *Geotechnical Engineering* **28(1)**: 89–119.

Wang Y, Fall M and Wu AX (2016) Initial temperature-dependence of strength development and self-desiccation in cemented paste backfill that contains sodium silicate. *Cement and Concrete Composites* **67**: 101–110, https://doi.org/10.1016/j.cemconcomp.2016.01.005.

Yilmaz E, Benzaazoua M, Belem T and Bussière B (2009) Effect of curing under pressure on compressive strength development of cemented paste backfill. *Minerals Engineering* **22(9–10)**: 772–785, https://doi.org/10.1016/j.mineng.2009.02.002.

How can you contribute?

To discuss this paper, please submit up to 500 words to the editor at journals@ice.org.uk. Your contribution will be forwarded to the author(s) for a reply and, if considered appropriate by the editorial board, it will be published as a discussion in a future issue of the journal.